^{232}Th neutron capture cross section

V.M. Maslov
Joint Institute for Nuclear and Energy Research
220109, Minsk-Sosny, Belarus

Abstract

Newest ^{232}Th neutron capture data are reproduced consistently with the total, fission and inelastic cross section data. Hauser-Feshbach-Moldauer theory is employed. Rigid rotator coupled channel model reproduces experimental neutron total cross section data. In keV-energy range capture cross section is defined mostly by the average radiative strength fuction $S_{\gamma o}$ value, in hundreds keV-energy range- by the energy dependence of the $S_{\gamma o}$, i.e., by the level density of ^{233}Th at low excitations, above ~1 MeV the (n,γn')-reaction competition plays a decisive role.

1 Introduction

Neutron capture data for ^{232}Th are far less investigated than those for the ^{238}U. Measured capture cross section data for ^{232}Th target nuclide are discrepant well beyond claimed errors. Recent measurements at IRMM(Geel) [1] and n_TOF Collaboration (CERN) [2] provide a fair basis for major improvement of the quality of the evaluated data files, since capture cross sections of ENDF/B-VI [3] and JENDL-3.3 [4] are quite discrepant with the newest measured data trends.

Newest measured capture cross section data for ^{232}Th [1, 2] are actually prompt gamma-ray measurements, they cover energy range of 4 keV- 140 keV [1] and 1 keV - 1 MeV [2]. However, these newest measured data are at variance with recent prompt gamma-ray measurements in the energy range from 5 to 225 keV by Wisshak et al. [5] and with the activation measurements by Karamanis et al. [6] at higher incident neutron energies up to ~2 MeV. Generally, data by Wisshak et al. [5] and by Karamanis et al. [6] define the lowest cross section level in the ~20-2000 keV energy range. At the higher extreme are the IRMM data [1] and n_TOF data [2], which are supported by the older activation measurements by Poenitz and Smith [7], Lindner et al. [8] and Anand et. al. [9]. Above $E_n \sim 150$ keV data by Kobayashi et al.[10] and renormalized in [11] data by Macklin [12] as well as data by Anand et al. [9] are compatible with newest IRMM [1] and n_TOF [2] data. Other data sets (see for details discussion in [13, 14]) in some cases are compatible with the newest data at $E_n \gtrsim 50$ keV, but at lower energies they predict ~10% lower cross section level.

The possibility to estimate capture cross section in a statistical model of compound nucleus reactions from 1 keV up to 5 MeV was investigated recently [13]. Our previous evaluation [13, 14] is quite compatible with the newest measured data [1, 2] below E_n ~50 keV and above 500 keV, but the precise fit of the newest data trend in between needs some adjustment of the statistical and optical model parameters.

Though neutron data base for ^{232}Th is much less expanded as that of ^{238}U, due to the theoretical modelling of capture cross sections [13], coupled with direct excitation of vibrational collective bands [15, 16], modelling of pre-fission neutron influence on prompt

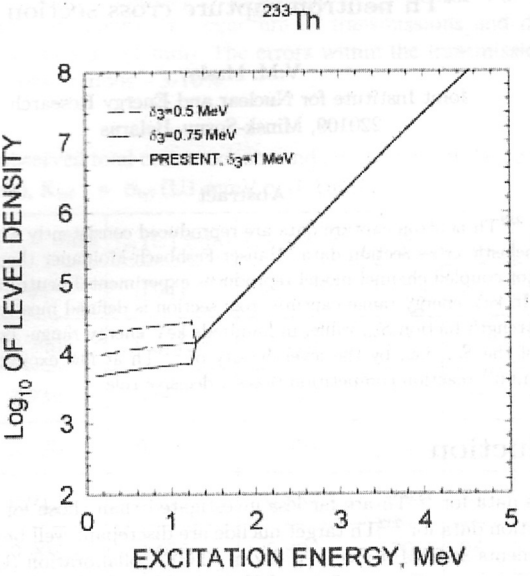

Figure 1: Level density of ^{233}Th

fission neutron spectra and multiplicities [17, 18], ^{232}Th evaluated neutron cross sections and secondary neutron spectra could be much improved [14, 19] and extended up to 200 MeV [20, 21, 22, 23, 24].

2 Statistical model

The statistical model of compound nucleus reactions as applied for the capture cross section analysis from $E_n \sim 1$ keV to 5 MeV is based on the average resonance parameters and consistent description of competing cross section data, i.e. total, elastic and inelastic scattering cross sections. We employed Hauser-Feshbach-Moldauer theory and coupled channel optical model, described elsewhere [13].

Neutron capture cross section is defined as

$$\sigma_{n\gamma}(E_n) = \frac{\pi\,\bar{\lambda}^2}{2(2I+1)} \sum_{lj J\pi} (2J+1) T_{lj}^{J\pi}(E_n) P_{\gamma\gamma}^{J\pi}(E_n) S_{n\gamma}^{lj J\pi}, \tag{1}$$

the compound nucleus radiative capture probability $P_{\gamma\gamma}^{J\pi}$ is

$$P_{\gamma\gamma}^{J\pi}(E_n) = \frac{T_{\gamma\gamma}^{J\pi}(U)}{T_f^{J\pi}(U) + T_n^{J\pi}(U) + T_\gamma^{J\pi}(U)}, \tag{2}$$

where $U = B_n + E_n$ is the excitation energy of the compound nucleus, B_n is the neutron binding energy, E_n is the incident neutron energy, $T_{lj}^{J\pi}$ are the entrance neutron transmission

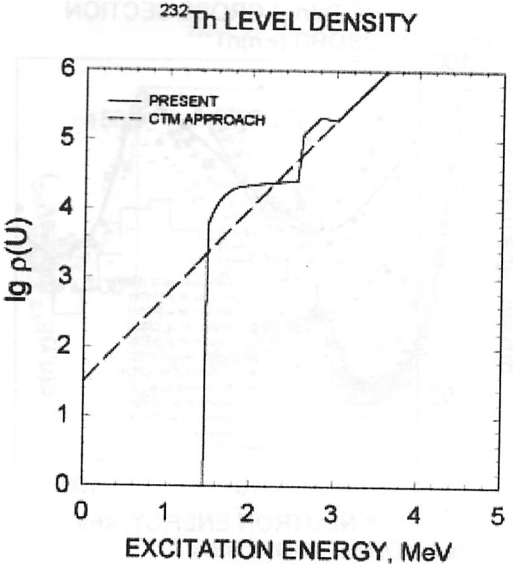

Figure 2: Level density of ^{232}Th

coefficients for the channel $(ljJ\pi)$, I is the target nucleus spin. Neutron capture probability $P^{J\pi}_{\gamma\gamma}(E)$ of the compound nucleus with excitation energy U for given spin J and parity π, depends on $T^{J\pi}_{\gamma\gamma}$, $T^{J\pi}_{\gamma}$, $T^{J\pi}_{n}$ and $T^{J\pi}_{f}$ transmission coefficients of the radiative capture, radiative decay, neutron scattering and fission channels, $S^{ljJ\pi}_{nx}$ denotes partial widths Porter-Thomas fluctuation factor.

The important item for the capture cross section calculation is ^{233}Th nuclide level density, it strongly influences the energy dependence of the radiative strength function $S_{\gamma o} = \langle\Gamma_\gamma\rangle / \langle D_{l=0}\rangle$ above $E_n \sim$100 keV, here $\langle\Gamma_\gamma\rangle$ is the average radiation width, $\langle D_{l=0}\rangle$ is average $s-$wave resonance spacing. In case of even-odd nuclei the partial contribution of $1-$quasiparticle states $\omega_{nqp}(U)$ to the total intrinsic state density $\omega_{qp}(U)$ produces "plateau" below three-quasiparticle excitation threshold U_3 (see Fig. 1) [13]. The arrows on the horizontal axis of Fig. 1 indicate the excitation thresholds of odd $n-$quasiparticle configurations. Nuclear level density $\rho(U) \sim K_{rot}(U)K_{vib}(U)\omega_{qp}(U)$, where $K_{rot}(U)$ and $K_{vib}(U)$ are factors of rotational and vibrational enchancement of the level density, is virtually independent of the excitation energy up to the three-quasiparticle excitation threshold U_3, since the intrinsic state density ($\omega_1 \sim g$) is constant. In this excitation energy region we model the level density as

$$\begin{aligned}\rho(U) &= T^{-1}(1 + 2(U - 0.5U_3))\exp((U_3 + \Delta_f - U_o - \delta_3)/T) \\ &\sim \exp((\Delta_f - U_o)/T).\end{aligned} \tag{3}$$

Above the three-quasiparticle states excitation threshold U_3 the constant temperature model is used, since the intrinsic state density here is virtually a smooth function of the excitation

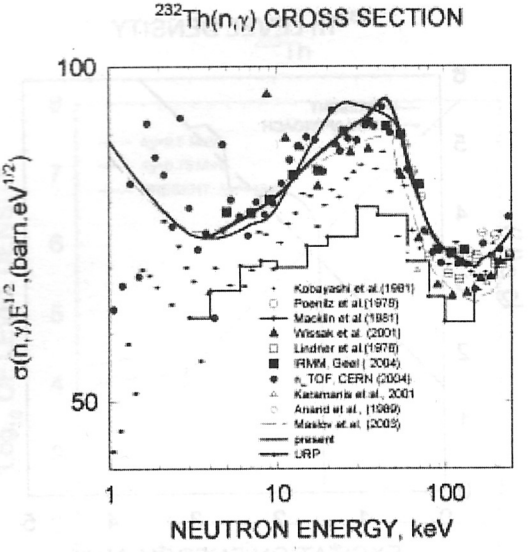

Figure 3: ^{232}Th(n,γ) cross section.

energy. The numerical values of parameter δ_3 =1 MeV is defined by fitting ^{232}Th capture cross section data.

At incident neutron energies higher than E_n ~1 MeV, the Moldauer [25] effect , i.e. the competition of neutron emission at the second cascade, i.e. after first γ-quanta emission should be included. Then "true" capture reaction cross section (n,$\gamma\gamma$), which competes with the (n,γn') reaction, is defined using transmission coefficient $T^{J\pi}_{\gamma\gamma}(U)$ defined in a two-cascade approximation as

$$T^{J\pi}_{\gamma\gamma} = \frac{2\pi C_{\gamma 1}}{3(\pi hc)^2}\int \varepsilon^2_\gamma \sigma_\gamma(\varepsilon_\gamma) \sum_{I=|J-1|}^{I=J+1} \rho(U-\varepsilon_\gamma, I, \pi)\frac{T^{I\pi}_\gamma}{T^{I\pi}_f + T^{I\pi}_{n'} + T^{I\pi}_\gamma} d\varepsilon_\gamma \ . \quad (4)$$

The last term of the integrand in Eq. (4) describes the competition of $\gamma-$ or neutron emission and fission at excitation energy $(U-\varepsilon_\gamma)$ after emission of first γ-quanta with energy ε_γ, $C_{\gamma 1}$ is the normalizing coefficient. That means radiative, neutron and fission transmission coefficients $T^{I\pi}_\gamma$, $T^{I\pi}_{n'}$ and $T^{I\pi}_f$ are defined at excitation energy $(U-\varepsilon_\gamma)$. The neutron emission after emission of first $\gamma-$quanta strongly depends on the ^{232}Th residual nuclide level density at excitations just above paring gap [26]. The competition of ^{232}Th(n,γn') reaction to the "true" capture reaction (n,$\gamma\gamma$) turns out to be dependent on the target nuclide ^{232}Th level density at excitations just above the pairing gap. Inelastic scattering cross section, actually its compound scattering component, helps to fix the ^{232}Th level density model parameters above the pairing gap U_2. Nuclear level density $\rho(U)$ of even-even nuclei above the pairing gap up to the four-quasiparticle excitation threshold is extracted by fitting total inelastic and fission cross section data of ^{232}Th. Present estimate of total level density for even nuclide

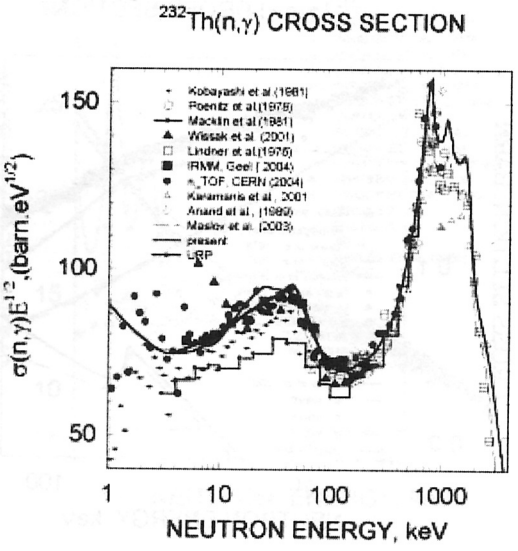

Figure 4: ^{232}Th(n,γ) cross section.

^{232}Th at equilibrium deformation is compared with the structureless constant temperature model approximation of $\rho(U)$ on Fig. 2. The arrows on the horizontal axis of Fig. 2 indicate the excitation thresholds of even $n-$quasiparticle configurations. Below the excitation threshold U_2, i.e. within pairing gap the constant temperature model fits cumulative number of ^{232}Th levels [27]. Actually the collective levels of ENSDF [27] are employed within pairing gap. We modelled the nuclear level density $\rho(U)$ of even-even nuclei above the pairing gap up to the four-quasiparticle excitation threshold as

$$\rho(U) = \rho(U_4 - \delta_4)/(1 + \exp((U_2 - U + \delta_a)/\delta_s)). \quad (5)$$

This estimate almost coincides with that obtained with Bose-gas modelling of intrinsic state density. The numerical values of δ_4 =0.3 MeV, $(\delta_4 \sim 0.5(U_4 - U_2)), \delta_a$ =0.1 MeV, $\delta_s = 0.1$ MeV parameters, for residual nucleus, defining shape of $\rho(U)$ are extracted by fitting total inelastic and fission cross section data of ^{232}Th. The other details of the model are described elsewhere [13].

3 Capture data analysis

Our previous evaluation [13, 14] is quite compatible with the newest measured data [1, 2] below E_n ~50 keV, small discrepancy around ~50 keV could be easily diminished by slight increase of thevalue of $p-$wave strength function S_1. Table 1 compares S_l neutron strength functions at 4 keV with those of [13, 14, 2, 1]. At higher energies, especially in the energy

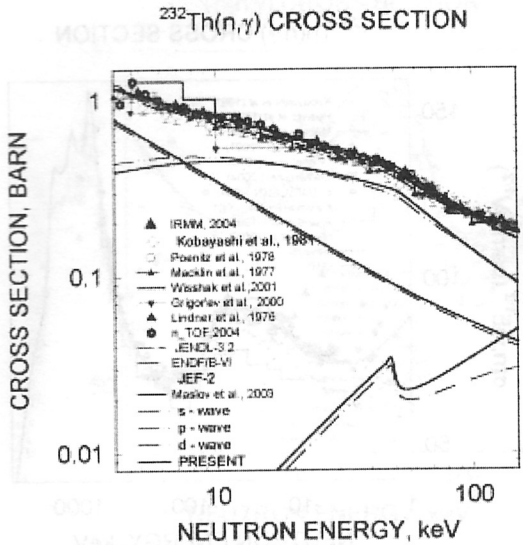

Figure 5: ^{232}Th(n,γ) cross section.

range of 50-500 keV the calculated curve remains much lower, it follows the data trend by Wisshak et al. [5] and is rather close to the data by Karamanis et al. [6].

The capture cross section level in the energy range of E_n ~50-500 keV is defined by the $S_{\gamma o} = \langle \Gamma_\gamma \rangle / \langle D_{l=0} \rangle$ radiative strength function value, once the $s-$ and $p-$ wave neutron strength functions S_0 and $S_1$are fixed by both averaging of the resolved resonance parameters and the total cross section description. There is an evidence that some $p-$wave resonances were assigned as $s-$resonances [13, 2]. The $s-$wave neutron resonance spacing may increase somewhat against the value of $\langle D_{obs} \rangle$ =17.385 eV [13, 14], while there is some evidence [1] that $\langle \Gamma_\gamma \rangle$ also may increase to 24.4 meV, against 21.3 meV, adopted in [13, 14]. The net effect might be that $S_{\gamma o}$ value will remain almost unchanged, or increase by~10% at most. Actually, the increase of the $S_{\gamma o}$ value by ~10% allows to describe the newest data [1, 2] trend above ~200 keV. Figures 3 and 4 show the comparison of measured capture data with present and previous [13, 14] calculations. Capture cross section, calculated with ENDF/B-format unresolved resonance parameters, is also shown. Then at lower energies the capture data fit will need a lowering of the S_1 neutron strength function value. To maintain a capture data fit in a E_n ~4–50 keV energy range the contribution of the $p-$wave should be decreased. To reproduce the energy dependence of the calculated capture cross section in the energy range of E_n ~50-500 keV the contributions of $d-$ and $f-$waves were increased, this was done by decrease by 0.5 MeV of the real volume optical potential, to V_R =45.222 MeV and increase by 0.02 of the hexadecapole deformation β_4 =0.091 of the coupled channel optical potential [13]. Figure 5 shows partial contributions of $s-$, $p-$ and $d-$wave channels to the observed capture cross section. Figure 6 shows total cross section data. The shift of the calculated cross section to the measured data by Grigoriev et al. [28] is evidenced.

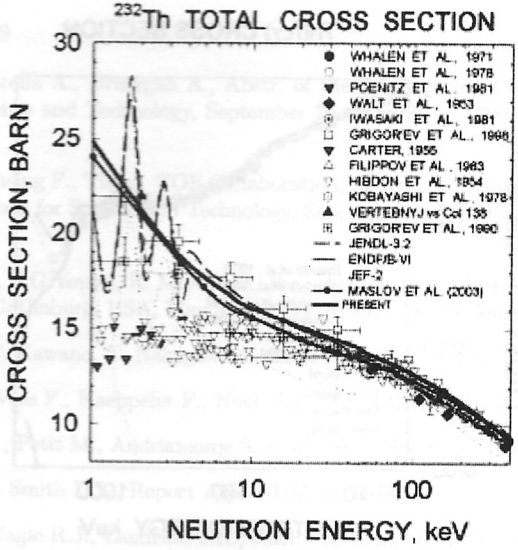

Figure 6: ^{232}Th total cross section.

Table 1
Neutron strength functions and average resonance perameters for ^{232}Th

	E_n, keV	$S_0 \times 10^{-4}$	$S_1 \times 10^{-4}$	$S_2 \times 10^{-4}$	Γ_γ	$\langle D \rangle$
present	4	0.9686	1.8569	1.4699	23.8	17.895
[13, 14]	4	0.94	2.15	1.15	21.3	17.895
[2]		0.66±0.02	1.3±0.02	0.4±0.01	24.4	16.6
[1]		0.935	1.84	1.18	24.4	17.28

Neutron strength functions S_0 , S_1 and S_2 change linearly in the energy ranges of 4-50 keV and 50-150 keV. At $E_n \sim$4, 50 and 150 keV they are equal to the calculated values. Other details of the modelling are described elsewhere [13, 14].

For still higher incident neutron energies $E_n \gtrsim$1 MeV, the $(n, \gamma n')$ reaction competition to the "true" capture $(n, \gamma\gamma)$ reaction cross section is rather strong, it essentially defines the capture cross section drop above $E_n \sim$1 MeV. Figure 7 shows the cross section of $(n, \gamma n')$ reaction and the cross section of $(n, \gamma x)$ reaction, which is the sum of $\sigma_{n,\gamma\gamma}$ and $\sigma_{n,\gamma n'}$ cross sections. The competition of $(n, \gamma f)$ reaction to the "true" capture $(n, \gamma\gamma)$ reaction is inessential for ^{232}Th$(n, \gamma\gamma)$ reaction due to low fission probability of ^{233}Th nuclide.Consistent description of the total, elastic and inelastic scattering cross section data up to $E_n \sim$5 MeV is also maintained.

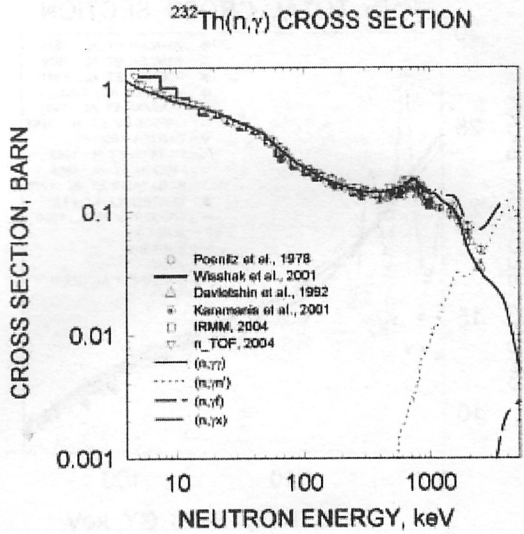

Figure 7: ^{232}Th capture cross section.

4 Conclusions

The statistical Hauser-Feshbach-Moldauer model calculation of neutron-induced reaction cross sections for ^{232}Th target nucleus shows a fair description of measured data base on ^{232}Th+n total, elastic, fission, capture, inelastic scattering reaction cross sections up to 5 MeV. Newest ^{232}Th neutron capture data in the energy range of 1 keV - 1 MeV [1, 2] are reproduced consistently with the total cross section data. Unresolved resonance parameters are obtained, which reproduce total, capture and inelastic cross sections from 4 keV up to 150 keV. Nucleon optical model potential for ^{232}Th is obtained, based on consistent analysis of differential elastic and inelastic scattering data and total cross section data, further tuning of the optical model potential parameters is obtained by fitting of the capture data in hundreds keV-energy range. Radiative strength function provides good capture cross section data description in 4 keV - 5 MeV energy region. However, further measurements are highly requested for the energy range from 1 MeV up to 5 MeV.

5 Acknowledgements

This work is supported by the International Atomic Energy Agency (Vienna, Austria) under Research Contract No. 12353.

References

[1] Volev K., Borella A., Brusegan A., Abstr. of the International Conference on Nuclear Data for Science and Technology, September 26 – October 1, 2004, Santa Fe, USA, p. 176.

[2] Aerts G., Gunsing F., The n_TOF Collaboration, Abstr. of the International Conference on Nuclear Data for Science and Technology, September 26 – October 1, 2004, Santa Fe, USA, p. 284.

[3] R.W.Roussin, P.G.Young, R. McKnight, Proc. Int. Conf. Nuclear Data for Science and Technology, Gatlinburg, USA, May 9-13, 1994, p. 692, J.K. Dickens (Ed.), ANS, 1994.

[4] K. Shibata, T. Kawano, T. Nakagawa et al., J. Nucl. Sci. Technol., 39, 1125 (2002).

[5] Wisshak K., Voss F., Kaeppeler F., Nucl. Sci. Eng., 137 (2001) 183.

[6] Karamanis D., Petit M., Andriamonje S. et al., Nucl. Sci. Eng., 139 (2001) 282.

[7] Poenitz W.P., Smith D.L., Report ANL-NDM-42, 1978.

[8] Lindner M., Nagle R.J., Landrum J.H., Nucl. Sci. Eng., 59 (1976) 381.

[9] Anand R.P., Jain H.M., Kailas S., et. al., Annals of Nucl. Energy, v.16(2), p.87, 1989.

[10] Kobayashi K., Fujita Y., Yamamuro N., Nucl. Sci. Techn., 18 (1981) 823.

[11] Macklin R.L., R.R. Winters Nucl. Sci. Eng., 78 (1981) 110.

[12] Macklin R.L.,Halperin J., Nucl. Sci. and Eng., 64 (1977) 849.

[13] Maslov V.M. et al., Nucl. Sci. and Eng., 143 (2003) 177.

[14] Maslov V.M. et al., INDC(BLR)-016, IAEA, Vienna, 2003.

[15] Maslov V.M. et al.,Proc. International Conference on Nuclear Data for Science and Technology, October 7-12, 2001, Tsukuba, Japan, p. 148, 2002.

[16] V. M. Maslov et al., Izvestiya Rossiskoi Akademi Nauk. Seriya Fizicheskaya, 67, 1599 (2003) .

[17] Maslov V.M. et al., Phys. Rev. C 68, 034607 (2004).

[18] Maslov V.M. et al. EuroPhysics Journal A, 18 (2003) 93.

[19] Maslov V.M., Nucl. Phys., A743 (2004) 236.

[20] V.M. Maslov, Nucl. Phys., A 717 (2003) 3.

[21] V.M. Maslov et al., Nucl.Phys. A, 736, 77 (2004).

[22] V.M. Maslov, Phys. Lett. B, 581, 55 (2004).

[23] V.M. Maslov, EuroPhysics Journal A, (2004), A, 21 (2004) 281.

[24] Maslov V.M., Nucl. Phys., in press.

[25] P.A. Moldauer, Proc.Conf. on Neutron Cross Sections and Technology, Washington, D.C., USA, March 22-24, 1966, p. 613-622, AEC (1966).

[26] V.M. Maslov, Proc. 9th Int. Symp. on Capture Gamma-Ray Spectroscopy and Related Topics, Budapest, Hungary, October 8-12, 676, Springer (1996).

[27] M. Shmorak, Nucl. Data Sheets, 36, 367 (1982).

[28] Grigor'ev Yu.V., Sinitsa V.V., Gundorin N.A., et. al., , VI International Seminar on Interaction of Neutrons with Nuclei, Dubna, Russia, May 13-16, 1998, p. 194, 1998.